Focusing properties of Azimuthally Polarized Lorentz Gauss Vortex Beam through a Dielectric Interface

Chokkalingam Saraswathi, [1] Lavanya Maruthasalam,[2] Mariyappan Udhayakumar, [*] [3] Zbigniew Jaroszewicz[4]

[1]*Department of Physics, Government Arts College, Dharmapuri, Tamilnadu, India*
[2]*Department of Physics, PSGR Krishnammal College for Women, Coimbatore, Tamilnadu, India, 641004*
[3]*Chikkanna Government Arts College, Tiruppur,*
[4]*National Institute of Telecommunications, Szachowa 1, 04-894 Warsaw, Poland*

Abstract—Tight focusing properties of azimuthally polarized Lorentz Gaussian vortex beam through a dielectric interface are numerically studied by vector diffraction theory. The focusing properties, such as spot size, depth of focus, and maximum intensity position, are numerically calculated by properly manipulating the Lorentz parameter with/without annular obstruction values. Thus, using annular obstruction, one can generate a highly confined focal spot of long focal depth when using an azimuthally polarized Lorentz Gaussian vortex beam.

In 1986, Ashkin reported that optical trapping of dielectric particles by a single-beam gradient force trap was demonstrated for the first time [1]. Since then, this new technology has found wide applications in manipulating various particles, such as micro-sized dielectric particles, neutral atoms, cells, DNA molecules, and living biological cells [2–6]. In this research, the incident light beam is focused in the vacuum. However, in many practical applications, an objective is used to focus an incident light beam through an interface between different media of different refractive indices. For example, in the case of optical trapping, a laser beam is focused through an interface between glass and water [7], and in the application of semiconductor inspection, light beams are focused from air onto a silicon substrate. In their research, the incident light is focused into a uniform medium of refractive index n. The theoretical method for studying the focusing of an electromagnetic wave through dielectric interfaces has been carried out [8–10]. A Lorentz beam array is an excellent model for exploring a coherent diode laser array, and detailed research on the propagation properties of a Lorentz beam array was presented by Zhou *et al.* [11]. The Lorentz beam can be regarded as a particular case of Lorentz–Gauss beams. With the spatial extension being the same, the angular spreading of a Lorentz–Gaussian distribution is higher than that of a Gaussian description [12]. If the radiation emitted by a single-mode diode laser goes through a spiral phase plate, it becomes a Lorentz–Gauss vortex beam. The wave-front phase of a Lorentz–Gauss vortex beam can be modulated by the spiral phase plate. The advantage of a Lorentz–Gauss vortex beam over the Lorentz–Gauss beam is that it has a twisted phase front and zero intensity in the center region of the beam profile. Owing to carrying the orbital angular momentum, a Lorentz–Gauss vortex beam has potential applications in optical micromanipulation, nonlinear optics, quantum information processing, etc. [12–15]. However, to the best of our knowledge, there are no papers studying the tightly focusing properties of azimuthally polarized Lorentz vortex beams through a dielectric interface.

A schematic diagram of the suggested method is shown in Fig. 1. The azimuthally polarized Hollow Gaussian beam is focused through a high NA lens system. Assume the interface between two dielectric media of refractive indices $n_1 = 1$ and $n_2 = 3.55$, such as focusing in air onto silicon substrate in the application of semiconductor inspection. The geometric focus of the objective without the interface is located at the origin O of the coordinate system. The distance between the interface and the geometric focus d is called probe depth [16].
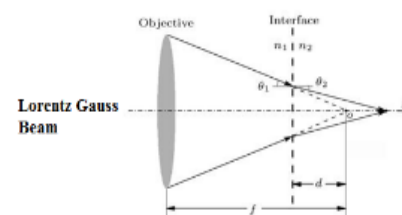
Fig .1. Scheme of an optical system.

In the focusing system, we investigated, the incident beam is the Lorentz beam, whose amplitude distribution of electric field is in the form of [12–15]:

$$A(\theta,\varphi) = \frac{C}{\omega_x \omega_y} \cdot \frac{1}{1+\cos^2\varphi\left(\sin^2\theta / NA^2\,\omega_x^2\right)} \cdot \frac{1}{1+\sin^2\varphi\left(\sin^2\theta / NA^2\,\omega_y^2\right)^2},$$

where ω_x, ω_y are parameters related to the beam width, C is chosen as constant, and NA is the numerical aperture of the incident beam. For azimuthally polarized beams, the

[*] E-mail: udhayaphy1985@gmail.com

Cartesian components of the electric field vector in the focal region then could be written as [16]:

$$E(r,\psi,z) = \begin{bmatrix} E_x(r,\psi,z) \\ E_y(r,\psi,z) \\ E_z(r,\psi,z) \end{bmatrix} = \frac{-iE_0}{\pi} \int_{\delta-\alpha}^{\alpha} \int_0^{2\pi} \exp[-ik_0\Phi(\theta_1,\theta_2)] \cdot$$

$$\cdot \sin\theta_1 \sqrt{\cos\theta_1} \, A(\theta_1) \cdot t_p [ik_2 z \cos\theta_2 + ik_1 r \sin\theta_1 \cos(\psi-\phi)] \cdot \begin{bmatrix} -\sin\phi \\ \cos\phi \\ 0 \end{bmatrix} d\phi \, d\theta_1,$$

where $k_i = n_i k_0$ is the wave number, $J_n(x)$ is the Bessel function of the first kind of order n, $\alpha = \arcsin(\text{NA})$ is the maximal angle determined by the NA of the objective; t_p is the amplitude transmission coefficients for parallel polarization states, which is given by the Fresnel equations:

$$t_p = \frac{2\sin\theta_2 \cos\theta_1}{\sin(\theta_1+\theta_2)\cos(\theta_1-\theta_2)}.$$

The function $\Phi(\theta_1,\theta_2)$ is given by equation $\Phi(\theta_1,\theta_2) = -d(n_1\cos\theta_1 - n_2\cos\theta_2)$, representing the so-called aberration function caused by the mismatch of the refractive indices n_1 and n_2. Here θ_1 and θ_2 are related by the well-known Snell law.
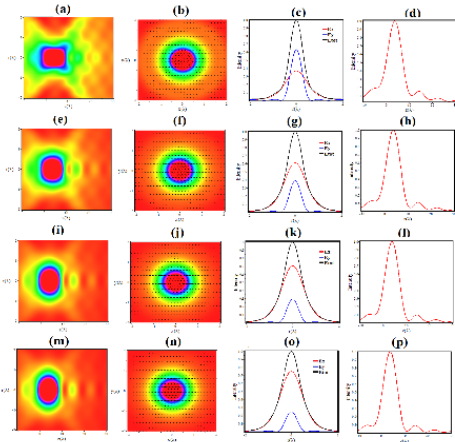
Fig. 2. Panels (a, e, i, m) show the r-z plot corresponding to δ=0, NA = 0.95, w_x = 0.3, and w_y = 0.3, 0.6, 0.9 and 1.2 respectively. Panels (b, f, j, n) show the corresponding intensity in the x-y plane. Panels (c, g, k, o) show the 2D intensity in the radial direction, and panels (d, h, i, p) show the corresponding axial intensity.

Figure 2 shows the focal structure generated for the azimuthally polarized Lorentz vortex beam with different Lorential parameters. It is clear from Fig. 2(a) that when ω_x=0.3 and ω_y =0.3, the generated focal structure is found to be not at focus (z=0), but it is shifted to 4λ. The FWHM of the focal spot is determined as 0.662λ from the radial intensity distribution measured at the point of maximum on axial intensity, and it is shown in Fig. 2(c). It is also observed from Fig. 2 that the E_y component is

more dominating than the E_x component, which is much broader than the E_y component. The x-y intensity distribution shown in Fig. 2(b) reveals that the electric field distribution is oriented mostly along the y-direction. The axial intensity calculated shows the DOF of the focal spot as 7.38λ and is shown in Fig. 2(d). Figure 2(e) shows that for ω_x =0.3 and ω_y =0.6, the focal spot further broadens in the radial direction due to the fact that the broader E_x component starts dominating E_y component, as shown in Fig. 2(g). The calculated FWHM of the focal spot around 0.804λ, and DOF of the generated focal spot around 7.22 λ are shown in Figs. 2(g) and 2(h), respectively. The intensity distribution in the x-y plane shows that the electric field vectors at the focus are more oriented along the x-direction, as shown in Fig. 2(f). Figures 2(i, j, k, l) represent the same characteristics as in Figs. 2(e, f, g, h), but for ω_y =0.9. It is observed that further increasing the Lorential parameter makes the E_x component more dominating and leads to a further increase in focal spot size. The FWHM of the focal spot is measured to be 0.867λ, and DOF is measured as 7.34λ. The same trend is observed for ω_y=1.2, and Fig. 2 (m) shows the enlargement of the focal spot in the radial direction with FWHM of the focal spot around 0.924λ and DOF around 7.46λ. Thus, increasing the Lorential parameter increases the foal spot size due to the dominating E_x component. It is also noted that the position of maximum intensity is located at 4λ for all the Lorential parameters considered.
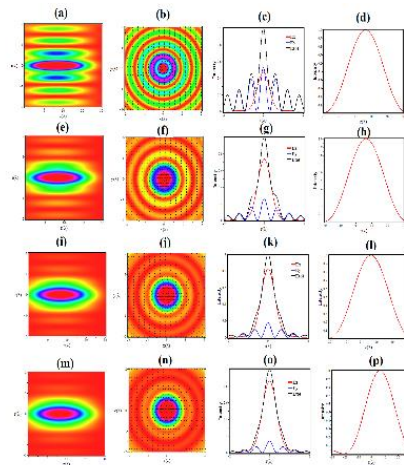
Fig. 3. The same characteristics as shown in Fig. 2 but obtained for δ=0.75.

Figure 3 shows the same characteristics as in Fig. 2 but obtained for δ=0.75. As evident from the 3D plots shown in Fig. 3, obtained for δ=0.75 and ω_y=0.3, generated a much confined focal spot with a large DOF. It is also observed that the position of the maximum intensity shifted to 6.4λ. The radial intensity calculated at the position of maximum intensity shows that the FWHM of the generated focal spot is reduced to 0.402λ with a much

dominating y-component with a large side lobe about 50% of the main lobe, and is shown in Fig. 3(c). The on-axial intensity calculated shows that the DOF of the generated focal spot is much improved to 25.2.4λ, as demonstrated in Fig. 3(d). However, for ω_y =0.6, the focal spot is 0.592λ, and DOF is around 24.7λ, as shown in Figs. 3(g) and 3(h), respectively. However, further increasing of ω_y to 0.9 and 1.2 slightly increased the focal spot to 0.686λ and 0.687λ, as shown in Figs. 3(k) and 3(o), respectively. The corresponding focal depths are 25.2.28λ and 25.2.22λ, as shown in Figs. 3(l) and 3(p), respectively. Thus, increasing the annular obstruction increases the focal depth and confines the focal spot. It is noted that the DOF and positional shift have little effect on the Lorential parameter.
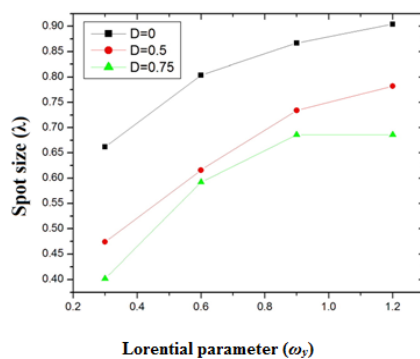
Fig. 4. Variation of Spot size with Lorential parameter.
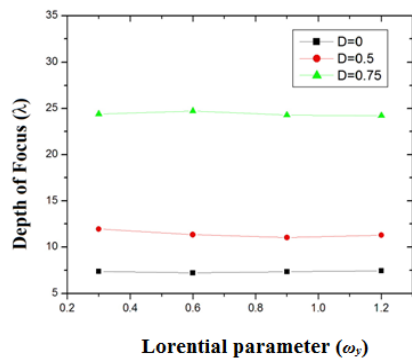
Fig.5. Variation of Depth of focus with Lorential parameter.
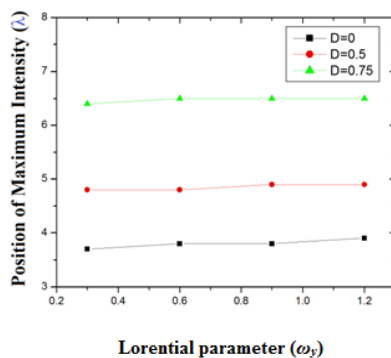
Fig. 6. Variation of Position of Maximum Intensity with Lorential parameter.

Figure 4 shows the spot size obtained corresponding to various values of the Lorential parameter. It is evident from Fig. 4 that the increase of the Lorential parameter increases the spot size. However, we get a minimum spot size when using annular obstruction with δ=0.75. Figure 5 shows the variation of DOF corresponding to different values of the Lorential parameter. It is visible that the DOF remains constant irrespective of the increase in the Lorential parameter. However, the DOF for the case with δ=0.75 was found to be maximum. Figure 6 shows the shift in the position of maximum intensity. It is also noted that the shift remains constant for all Lorential parameters and is found to be maximum for δ=0.75.

Thus, on the whole, for azimuthally polarized vortex beam with different Lorential parameter, the spot size and the depth of focus increases with an increase in Lorential parameter. In contrast, the position of maximum intensity remains the same. In the case of using annular obstructions of δ=0.5 and δ=0.75, the focal spot increases with an increase in the Lorential parameter. However, it is found to be much less than the unobstructed case. Thus, using annular obstruction, one can generate a highly confined focal spot of long focal depth when using an azimuthally polarized Lorentz Gaussian vortex beam.

References

[1] A. Ashkin *et al.,* Opt. Lett. **11**, 288 (1986).
[2] A. Ambardekar, Y.Q. Li, Opt. Lett. **30**, 1797 (2005).
[3] P. Zemánek, C.J. Foot, Opt. Commun. **146**, 119(1998).
[4] S.M. Block *et al.,* Nature **348**, 348 (1990).
[5] D.E. Smith*et al.,* Nature **413**, 748 (2001).
[6] L. Oroszi *et al.,* Phys. Rev. Lett. **97**, 058301 (2006).
[7] D.P. Biss, T.G. Brown, Opt. Express **9**, 490 (2001).
[8] P. Török *et al.,* J. Opt. Soc. Am. A **12**, 2136 (1995).
[9] S.H. Wiersma *et al.,* J. Opt. Soc. Am. A **14**, 1482 (1997).
[10] L.E. Helseth, Opt. Commun. **191**, 161 (2001).
[11] P. Zhou *et al.,*Appl. Opt. **49**, 2497 (2010).
[12] O.E. Gawhary, S. Severini, J. Opt. A: Pure Appl Opt **8**, 409 (2006).
[13] J. Yang *et al.,* Proc. SPIE **6824**, 68240 A (2007).
[14] O.E. Gawhary, S. Severini, Opt. Commun. **269**, 274 (2007).
[15] H. Yu, L. Xiong, B. Lü, Optik **121**,1455(2010).
[16] Z. Zhang, J. Pu, X. Wang, Chin. Phys. Lett. **25**, 1664 (2008).